PERGAMON

International Journal of Solids and Structures 38 (2001) 1935–1942

INTERNATIONAL JOURNAL OF SOLIDS and STRUCTURES

www.elsevier.com/locate/ijsolstr

Dynamic ductile fracture of 7075-T6 – an experimental analysis

Matthew T. Kokaly *, Jonghee Lee [1], Albert S. Kobayashi

Department of Mechanical Engineering, University of Washington, Seattle, WA 98195-2600, USA

Received 20 August 1999; in revised form 27 December 1999

Abstract

Dynamic moiré interferometry fringes surrounding a rapidly propagating crack in single edge notched, 7075-T6 aluminum specimen of 1.6 mm thickness were used to compare directly the T_ε^*-integral values associated with a near-crack integration contour, the crack-tip opening angles and the elastic strain energy release rate, G. While T_ε^* reached a steady state value and remained constant at the terminal crack velocity, G followed the well-known gamma curve and varied with the crack driving force at the terminal velocity. This limited result may be an indication of the inadequacy in linear elastic fracture mechanics characterization of dynamic ductile fracture. © 2001 Elsevier Science Ltd. All rights reserved.

Keywords: Dynamic fracture; Ductile fracture; T_ε^* integral; CTOA

1. Introduction

The voluminous literature on experimental studies of dynamic fracture over the past thirty years have been based mostly on linear elastic fracture mechanics (LEFM). One of the heuristic justifications for the use of LEFM to interpret dynamic fracture of thick ductile materials, such as A533B steel and 2024-T3 aluminum, was the cleavage fracture surface exhibited by such material. An early experimental justification on the use of LEFM was made by Kobayashi and Engstrom (1967) who used a single frame, ultra-high speed camera and geometric moiré to record the transient displacement fields in fracturing 7075-T6 and 7178-T6 aluminum alloy. The resultant transient crack-tip strain fields varied with $1/r^{(1/2)}$ in contrast to the higher strain singularity of the corresponding static crack-tip strain field. The results suggested that dynamic ductile fracture with a relatively high crack velocity of 10–20% of the Rayleigh wave velocity can be modeled by dynamic LEFM.

While dynamic fracture in the presence of small scale yielding has been amply characterized by the dynamic toughness, K_{ID}, no comparable fracture parameter has been definitively identified for dynamic ductile fracture. The J integral, which is widely used to identify the onset of ductile fracture, loses its path independence with crack extension due to the large scale unloading in the trailing wake of the propagating crack. In addition, the required HRR field no longer exists. These two results preclude the use of the

* Corresponding author.

[1] Presently in the Republic of Korea, Air Force Headquarters, Chungnam 320-910, South Korea.

PII: S0020-7683(00)00144-X

J integral as a characteristic crack-tip parameter. One proposed ductile fracture parameter is the T_ε^* integral (Stonesifer and Atluri, 1982; Atluri et al., 1984) which is a *near-field* integral based on the incremental theory of plasticity and reaches a steady state value under stable crack growth. This T_ε^* varies with the near-field integration contour and should be evaluated near the crack tip if it is to be considered a crack-tip parameter. However, once the near field integration contour Γ_ε is specified, the general form of the T^* integral (Nikishkov and Atluri, 1987), which incorporates Γ_ε in the integration contour, is path independent regardless of the size of the outer contour. Thus, unlike the J integral, the T^* integral is a path-independent integral in the presence of large scale yielding and unloading.

The ductile fracture criterion considered in this paper is the T_ε^* integral which was used successfully by Omori et al. (1998) and their colleagues in analyzing mode I, stable ductile crack growth in thin aluminum fracture specimens.

2. T_ε^*-integral criterion

The T_ε^* integral for a stationary crack identical to the popular J integral is characterized by the deformation theory of plasticity. However, for a quasi-statically or dynamically extending crack, where the deformation theory of plasticity is no longer valid, T_ε^* and J integral differ substantially. In order to account for the prior history effect, the integration contour for the T_ε^* integral extends together with the extending crack (Okada and Atluri, 1999a). The incremental T_ε^*, i.e., $\Delta T_{\varepsilon,}^*$ within a given stationary but elongated integration contour are then summed from the initiation of crack extension to its current crack-tip location consistent with the incremental theory of plasticity as shown by Brust et al. (1985). By confining the integration contour, Γ_ε, to the vicinity of a traction-free crack and by using the stress/strain fields generated by the incremental theory of plasticity. Pyro et al. (1995) have shown, through numerical experiments, that T_ε^* can be computed by the current T_ε^* without the need to sum ΔT_ε^* for each incremental crack extension. Moreover, the trailing portion of the contour integral can be ignored due to the vanishing resultant surface traction acting at such a near-crack contour (Okada and Atluri, 1999b). The nearness, ε, is set to the thickness of the specimen in order to guarantee a state-of-plane stress along the integration contour.

Since the contour integration no longer involves the unloaded regions, the contour integral ahead of the crack tip can now be evaluated by using the deformation theory of plasticity as this frontal region is dominated by the loading process. As a result, not only is the experimentally impractical procedure of evaluating ΔT_ε^* avoided but T_ε^* can now be determined directly from the measured displacement field surrounding a partial contour near and in front of the crack tip. This is a fortunate approximation since the state of stress based on the incremental theory of plasticity cannot be readily computed from the measured displacement and strain fields in the trailing crack wake region.

For a straight crack which is subjected to a self-similar straight crack propagation,

$$T_\varepsilon^* = \int_{\Gamma_\varepsilon} \left[W n_k - s_{ij} n_j u_{i,k} \right] \mathrm{d}\Gamma \tag{1},$$

where W is the strain energy density and $i, j, k = 1, 2$. The indices 1 and 2 represent the Cartesian coordinates parallel and perpendicular to the straight crack. Since the direction normal, $n_k = 0$, and the stresses, $s_{12} = s_{22} = 0$, the integrand in Eq. (1) vanishes in the trailing wake of the crack when Γ_ε is very close to the traction-free crack.

3. Crack-tip opening angles criterion

The critical crack-tip opening angles (CTOA) criterion assumes that the stable crack growth occurs when an angle made by a point on the upper surface of a crack, the crack tip, and a point on the lower surfaces

reaches a critical value. For convenience, a point 1 mm behind the crack tip has been used (Dawicke et al., 1995; Omori et al., 1998). Extensive experimental results from thin aluminum fracture specimens have shown that after an initial transient period, the CTOA remains constant throughout mode I stable crack growth (Dawicke et al., 1995; Dawicke et al., 1997). Moreover, a two dimension, elastic–plastic FE simulation of stable crack growth based on the CTOA criterion correctly predicted the load versus crack opening displacement (COD) relations and the mode I crack extension histories of the fracture specimens. A similar constant CTOA in dynamic fracture is sought in this study.

4. Method of approach

Dynamic T_{ε}^{*} has been previously determined experimentally using the laser caustic method by Nishioka et al. (1991). In this study, dynamic moiré interferometry, which not only yielded the dynamic T_{ε}^{*} but also the dynamic CTOA was used to determine the transient displacement fields perpendicular and parallel to the running crack in 7075-T6 aluminum alloy, single edge notch (SEN) specimen. The SEN specimen, as shown in Figs. 1 and 2, was either fatigue precracked or blunt notched for low and high crack velocity tests, respectively. A steep moiré grating with a low spatial frequency of 40 lines/mm on a mirror finished specimen surface (Wang et al., 1994) was used due to the presence of large scale plastic yielding. Four frames of the moiré fringe patterns corresponding to either the vertical or horizontal displacements were recorded by an IMACON 790 camera. The framing rate was also fixed to either 10,000 or 100,000 frames per second. As a result, multiple recordings of identically loaded SEN specimens at different delay timings were used to capture the entire fracture event that lasted about 1.2 ms. Despite all efforts to generate reproducible tests, no two dynamic fracture tests are identical and thus the final composite fracture event was constructed with due consideration of the load-times histories and the varying crack opening profiles of each fracture test.

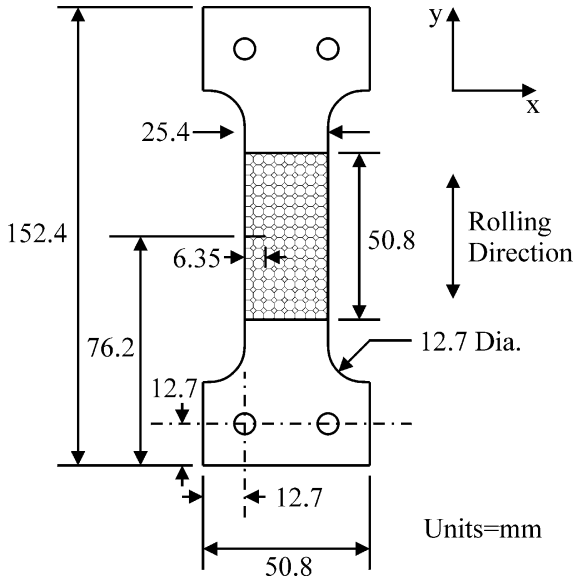

Fig. 1. Aluminum 7075-T6 SEN specimen.

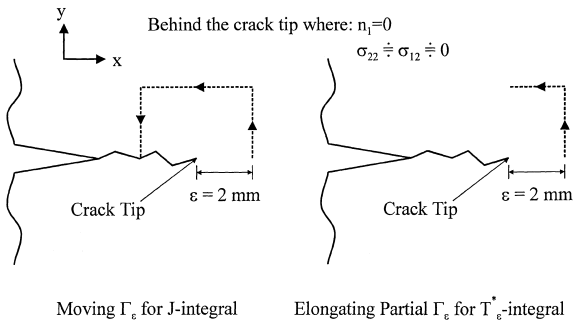

Fig. 2. Integration contours.

The complete displacement field was then used to compute the T^*_ε integral according to the procedure of Okada and Atluri (1999a). By neglecting the contour integral behind the propagating crack (Okada and Atluri, 1999b), only a partial near-crack contour at $\varepsilon = 2$ mm from the crack was used in the integration process thus simplifying the T^*_ε computation. The measured crack-tip displacement field was used to compute the CTOA and the LEFM-based strain energy release rate, G.

5. Results

Typical dynamic moiré fringes patterns associated with the propagating crack are shown in Fig. 3. Crack velocities of about 35 and 300 m/s were observed in the fatigue-precracked and blunt-notched specimens, respectively. The later crack speed is about 10% of the Rayleigh wave speed where Lee (1996) demonstrated, through numerical experiments, that the inertia effect resulted in a 10% increases in the static J values. Similar difference is expected between the static and dynamic T^*_ε values. Since the inertia terms in the J and T^*_ε integrals cannot be evaluated experimentally, the static formula of Eq. (1) was used to evaluate a pseudo-dynamic T^*_ε value.

As mentioned previously, a multitude of tests were assembled to construct a continuous crack propagation history. The successive crack opening profiles associated with these different tests is shown in Fig. 4. A remnant of the blunting of the fatigued crack tip prior to rapid crack propagation is evident throughout the entire crack propagation history. This initial crack-tip blunting is qualified in Fig. 5 which shows the

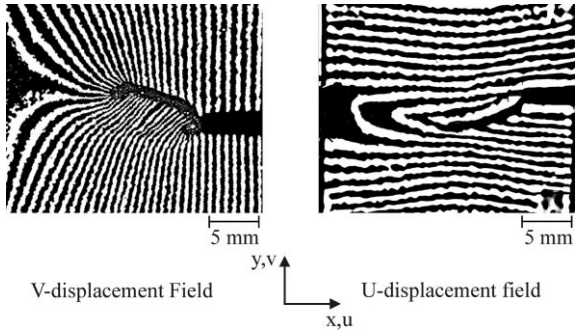

Fig. 3. Dynamic moiré patterns of fracturing 7075-T6 aluminum SEN specimens.

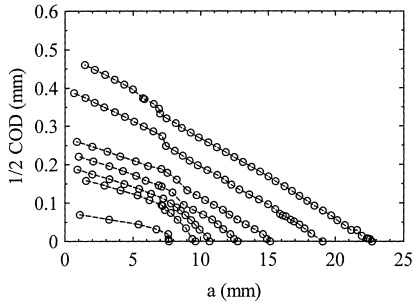

Fig. 4. Variations in crack opening with crack extension.

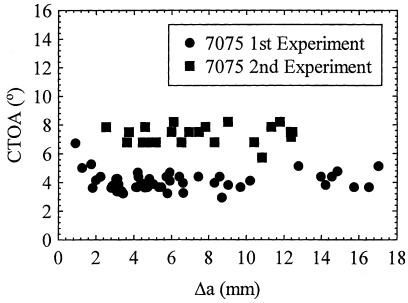

Fig. 5. CTOA variations with crack extension.

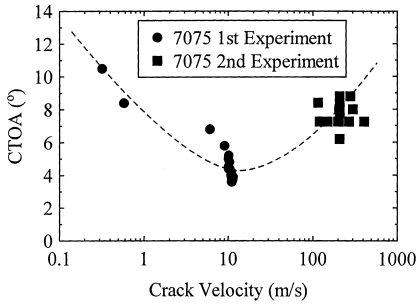

Fig. 6. CTOA variation with crack velocity.

CTOA dropping from its initial high value to a constant angle of 4° with crack extension in the first series of experiment. The data identified as the *first series* is from Lee et al. (1999) using fatigue-precracked specimens and the *second series* refers to the data from the blunt-notched specimens in this paper. The steady state CTOA in the second series is 7.5° higher. When the CTOA is plotted in terms of the crack velocity in Fig. 6, it passes through a minimum value at an intermediate crack velocity of about 100 m/s. This result is analogous to the dynamic fracture toughness versus crack velocity results for non-isothermal dynamic fracture of 2.25 Cr–1 Mo pressure vessel steel (Dally and Berger, 1993).

In contrast to the above-mentioned CTOA variation, the T_{ε}^{*} of the first and second series of tests followed the same trend of the quasi-static tests (Omori et al., 1998) where it gradually increased with the crack extension and reached separate steady values. When plotted in terms of the crack velocity, the

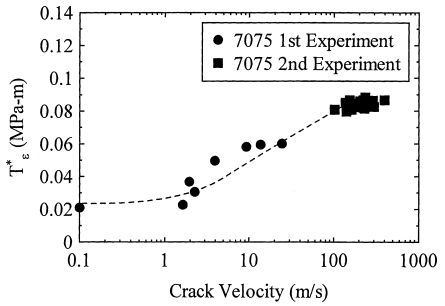

Fig. 7. T^*_ε versus crack velocity.

combined first and second series of tests, T^*_ε increased with increasing crack velocity and eventually leveled off at a terminal velocity of about 300 m/s as shown in Fig. 7.

6. Discussion

The literature on dynamic fracture shows that the LEFM-based dynamic strain energy release rate, G_{ID} with respect to crack velocity of somewhat brittle material exhibit a characteristic gamma-shaped curve. To check this conclusion, the CTOD at a crack-tip distance of $r = 1$ mm was used to compute the dynamic fracture toughness, K_{ID}, and hence the strain energy release rate, G_{ID}, based on LEFM for the first and second series of dynamic fracture tests of 7075-T6 aluminum specimens. The same procedure was also used to compute the G_{ID} for the blunt-notched 7075-T6 SEN specimens of Kobayashi and Engstrom (1967). An assembly of these three tests yielded the characteristic gamma-shaped G_{ID} versus crack velocity relation of Fig. 8.

The distinct difference in the G and T^*_ε responses at the terminal velocity suggests that the traditional practice of characterizing dynamic fracture of somewhat ductile material through the G_{ID} versus crack velocity relation based on LEFM could be misleading. The LEFM approach results in a terminal velocity, which is insensitive to the variation in the driving force, G_{ID}, while the T^*_ε approach based on elastic–plastic fracture mechanics (EPFM) suggests that the terminal crack velocity is a consequence of the saturation of the dissipated plastic energy.

Both the T^*_ε and CTOA, which are being considered for stable crack growth criteria, can also be considered as likely criteria for dynamic ductile fracture. CTOA, by definition, is a local crack-tip pa-

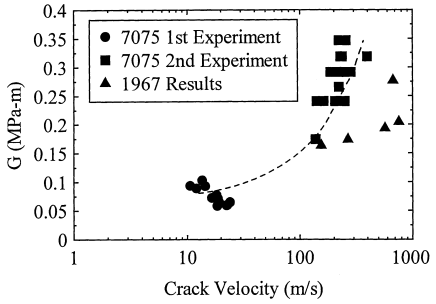

Fig. 8. G_{ID} versus crack velocity.

rameter which exhibited a precipitous drop at the initial phase of rapid crack propagation in fatigue-precracked 2024-T3 aluminum SEN specimens. Dawicke et al. (1995) attributed this drop to the crack front tunneling prior to crack extension. However, the blunt-machine-notched 7075-T6 SEN (second series) specimens in this study did not exhibit the initial high CTOA. Thus, the initial high value in CTOA in the fatigue-precracked SEN specimens is probably due to crack-tip blunting prior to crack extension.

7. Conclusions

Both the T_ε^*-integral and CTOA remained constant during the dynamic fracture event involving crack acceleration. The T_ε^* or the CTOA criteria proposed for stable crack growth could be used to characterize rapid crack propagation in ductile material.

The traditional G_{ID} versus crack velocity relation for characterizing dynamic ductile fracture of somewhat ductile material requires further investigation based on EPFM.

Acknowledgements

This work was supported by Office of Naval Research Contract N0001489J1276.

References

Atluri, S.N., Nishioka, T., Nakagaki, M., 1984. Incremental path independent integrals in inelastic and dynamic fracture mechanics. Engineering Fracture Mechanics 20, 209–224.

Brust, F.W., Nishioka, T., Atluri, S.N., Nakagaki, M., 1985. Further studies on elastic-plastic stable fracture utilizing T^* integral. Engineering Fracture Mechanics 22, 1079–1103.

Dawicke, D.S., Sutton, M., Newman, J.C., Bigelow, C.A. 1995. Measurement and analysis of critical CTOA for thin-sheet aluminum alloy materials. In: Erdogan, F. (Ed.), Fracture Mechanics, vol. 25. ASTM STP 1220, pp. 358–379.

Dawicke, D.S., Piascik, R.S., Newman, J.C. Jr., 1997. Prediction of stable tearing and fracture of 2000 series aluminum alloy plate using a CTOA criterion. In: Piascik, R.S., Newman, J.C. Jr., Dowling, N.E. (Eds.), Fatigue and Fracture Mechanics, vol. 27. ASTM STP 1296, pp. 90–104.

Dally, J.W., Berger, J.R., 1993. The role of the electrical resistance strain gage in fracture research. In: Epstein, J.S. (Ed.), Experimental Techniques in Fracture, SEM1–40.

Kobayashi, A.S., Engstrom, W.L., 1967. Transient analysis in fracturing aluminum plates. JSME Semi-International Symposium, 172–181.

Lee, J. 1996. Fracture Analysis of a Propagating Crack in a Ductile Material. A Ph.D. Thesis submitted to the University of Washington.

Lee, J., Kokaly, M.T., Kobayashi, A.S., 1999. Dynamic ductile fracture of aluminum SEN specimens: an experimental-numerical analysis. International Journal of Fracture 93, 39–50.

Nikishkov, G.P., Atluri, S.N., 1987. An equivalent domain integral method for computing crack-tip integral parameters in non-elastic, thermo-mechanical fracture. Fracture Mechanics 26, 851–867.

Nishioka, T., Sakai, K., Murakami, T. Matsuo, S., Sakakura, K. 1991. Measurement of nonlinear fracture parameter T integral under impact loading using laser caustic method. Transactions of 11th International Conference on Structure Mechanics in Reactor Technology, G13/1. Tokyo, pp. 321–326.

Okada, H., Atluri, S.N., 1999a. Further studies on the characteristics of the T_ε^* integral: plane stress stable crack propagation in ductile materials. Computational Mechanics 23, 339–352.

Okada, H., Atluri, S.N. 1999b. Direct evaluation of T_ε^* integral evaluation from experimentally measured near-tip displacement field for a plate with stably propagating crack, submitted for publication.

Omori, Y., Kobayashi, A.S., Okada, H., Ma, L., Atluri, S.N., Tan, P.W., 1998. T^* integral as a crack growth criterion. Mechanics and Materials 28, 147–154.

Pryo, C.R., Okada, H., Atluri, S.N., 1995. An elastic–plastic finite element alternating method for analyzing wide-spread fatigue damage in aircraft structures. Computational Mechanics 16, 61–68.

Stonesifer, R.C., Atluri, S.N., 1982. On the study of the $(\Delta T)_c$ and C^* integrals for fracture analysis under non-steady creep. Engineering Fracture Mechanics 16, 625–643.

Wang, F.X., May, G.B., Kobayashi, A.S., 1994. Low-spatial frequency steep geometric grating for use in moiré interferometry. Optical Engineering 33 (4), 1125–1131.